

Additive singular high-order complete vector functions for FEM and MoM applications to 2D and 3D sharp-wedge structures

*Original*

Additive singular high-order complete vector functions for FEM and MoM applications to 2D and 3D sharp-wedge structures / Lombardi, Guido; Graglia, Roberto. - ELETTRONICO. - 1:(2009), pp. 1-4. ( IEEE AP-S International Symposium and URSI National Radio Science Meeting Charleston, SC (USA) June 1-5, 2009) [10.1109/APS.2009.5171541].

*Availability:*

This version is available at: 11583/2297814 since:

*Publisher:*

IEEE

*Published*

DOI:10.1109/APS.2009.5171541

*Terms of use:*

This article is made available under terms and conditions as specified in the corresponding bibliographic description in the repository

*Publisher copyright*

(Article begins on next page)

# Additive singular high-order complete vector functions for FEM and MoM applications to 2D and 3D sharp-wedge structures

Guido Lombardi, Roberto D. Graglia  
Dipartimento di Elettronica, Politecnico di Torino, Torino, Italy  
E-mail: [guido.lombardi@polito.it](mailto:guido.lombardi@polito.it), [roberto.graglia@polito.it](mailto:roberto.graglia@polito.it)

## Introduction

The research results obtained by our group on numerical modeling of the diffraction effects due to abrupt material or geometrical discontinuities of electromagnetic structures are summarized. High order polynomial vector bases are often used to numerically model EM problems [1], but polynomial approximations spoil the convergence properties of the used finite method whenever the physical quantities have singular and/or irrational algebraic behavior in wedge regions. Our specially derived sub-sectional singular curl- and divergence-conforming vector bases incorporate the edge conditions of penetrable or conducting wedges, and yields to high precision results without requiring the use of dense meshes and/or local mesh refinements.

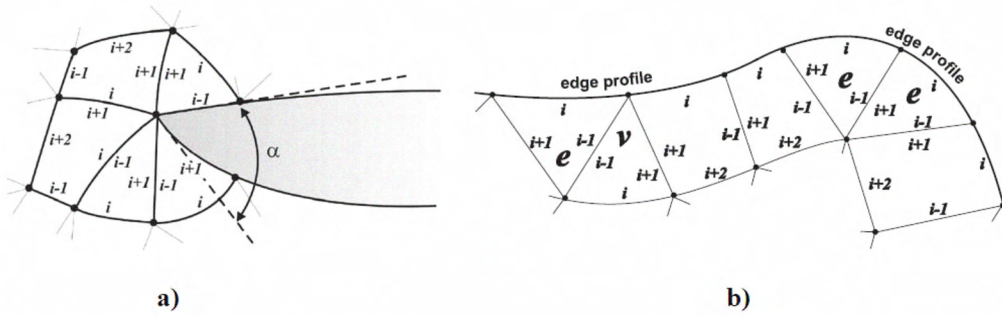


Fig. 1. a) 2D-FEM applications: cross-sectional view of the region around a sharp, but curved wedge of aperture angle  $\alpha$  meshed with curved curl-conforming elements. The sharp-edge elements are those attached to the sharp-edge vertex. b) 3D-MoM applications: edge singularity quadrilaterals and edge (e) and vertex (v) singularity triangles with the local edge numbering scheme used for the definition of the singular divergence-conforming functions.

## Requirements, Bases Definition and Numerical Validation

With reference to Fig. 1, our singular vector bases at the lowest singular order satisfy the following requirements [2-8] (where case A refers to the singular curl-conforming elements for 2D-FEM applications of Table I, and case B is relative to the divergence-conforming elements for 3D-MoM applications of Table II):

- they are complete to the regular zeroth order (A and B case);
- they are compatible to adjacent zeroth-order regular elements attached to the nonsingular edges, and compatible to adjacent singular elements of the same order attached to the other edges (A and B case);
- they model the static singular-behavior of the transverse EM fields (in case A), and the singular behavior of the current and charge density along the edge profile (in case B);

- they model the dynamic non-singular irrational algebraic behavior of the EM fields (in case A), and model the singular irrational algebraic behavior of the current normal to the edge profile (in case B).

Notice that for the numerical solution of surface integral equations (MoM applications) we define two type of singular triangles: the edge (e) and the vertex (v) singular triangle; the latter is considered as the appropriate element filler. To properly model the regular and the singular part of the physical quantities excited in the wedge region, we expand the unknown vectors by use of an additive scheme, i.e. we use the regular and the singular bases altogether on the same singular element. The bases are reported in Table I and II. Singular bases of this kind, complete to arbitrarily higher [p, s]-order are described in a unified and consistent manner for curved quadrilateral and triangular elements in [5], [7]. The singular bases guarantee normal (or tangential) continuity along the edges of the elements allowing for the discontinuity of tangential (or normal) components, adequate modeling of the divergence (or curl), and removal of spurious solutions. These bases provide more accurate and efficient numerical solutions for problems modeled by partial differential equations or by surface integral equations. Several test-case problems are considered in [5], [7], and new results for the 3D MoM-case will be discussed and presented at the conference, together with further details on how to implement the singular elements in FEM and MoM codes.

TABLE I  
LOWEST-ORDER CURL-CONFORMING BASES

Triangular Bases, with subscripts counted modulo 3, and $i = 1, 2$ or 3	
Basis Functions	Surface Curls
Regular Functions $\Omega_{\beta}(\mathbf{r}) = \xi_{\beta+1} \nabla \xi_{\beta-1} - \xi_{\beta-1} \nabla \xi_{\beta+1}$ for $\beta = i, i \pm 1$	$\nabla \times \Omega_{\beta}(\mathbf{r}) = 2 \hat{\mathbf{n}} / \mathcal{J}$ for $\beta = i, i \pm 1$
Wedge Functions ${}^0\Omega_{i\pm 1}(\mathbf{r}) = \nabla [\xi_{i\mp 1} (1 - \chi^{\nu-1})]$ ${}^{\nu}\mathbf{U}_i(\mathbf{r}) = (1 - \nu) (\chi^{\nu} - 1) \Omega_i(\mathbf{r})$ with $\chi = 1 - \xi_i$	$\nabla \times {}^0\Omega_{i\pm 1}(\mathbf{r}) = 0$ $\nabla \times {}^{\nu}\mathbf{U}_i(\mathbf{r}) = (1 - \nu) \frac{[(2 + \nu)\chi^{\nu} - 2]}{\mathcal{J}} \hat{\mathbf{n}}$ with $\chi = 1 - \xi_i$
Quadrilateral Bases, with subscripts counted modulo 4, and $i = 1, 2, 3$ or 4	
Basis Functions	Surface Curls
Regular Functions $\Omega_{\beta}(\mathbf{r}) = \xi_{\beta+2} \nabla \xi_{\beta-1}$ for $\beta = i, i + 2, i \pm 1$	$\nabla \times \Omega_{\beta}(\mathbf{r}) = \frac{\hat{\mathbf{n}}}{\mathcal{J}}$ for $\beta = i, i + 2, i \pm 1$
Wedge Functions ${}^0\Omega_i(\mathbf{r}) = (\xi_j^{\nu} - \xi_j) \nabla \xi_i + (\nu \xi_j^{\nu-1} - 1) \Omega_i(\mathbf{r})$ ${}^0\Omega_j(\mathbf{r}) = (\xi_i^{\nu} - \xi_i) \nabla \xi_j - (\nu \xi_i^{\nu-1} - 1) \Omega_j(\mathbf{r})$ ${}^{\nu}\mathbf{U}_{\beta}(\mathbf{r}) = (1 - \nu) (\xi_{\beta+2}^{\nu} - 1) \Omega_{\beta}(\mathbf{r}), \beta = i, j$ with $j = i + 1$	$\nabla \times {}^0\Omega_{\beta}(\mathbf{r}) = 0$ $\nabla \times {}^{\nu}\mathbf{U}_{\beta}(\mathbf{r}) = (1 - \nu) \frac{[(1 + \nu)\xi_{\beta+2}^{\nu} - 1]}{\mathcal{J}} \hat{\mathbf{n}}$ for $\beta = i, j$ and with $j = i + 1$
$\mathcal{J}$ indicates the element Jacobian and $\hat{\mathbf{n}}$ is the unit vector normal to the element [1].	

### Acknowledgment

This work is supported by NATO in the framework of the Science for Peace Programme under the grant CBP.MD.SFPP 982376 - Electromagnetic Signature of Edge-Structures for Unexploded Ordnance Detection.

TABLE II  
LOWEST-ORDER DIVERGENCE-CONFORMING BASES.

	Basis Functions	Surface Divergences <sup>♡</sup>	Dependency Relations
Quadrilateral Base The subscripts are counted modulo 4, for $i = 1, 2, 3$ or 4	Regular Functions [4] $\Lambda_\beta(\mathbf{r}) = \frac{\xi_{\beta+2} \ell_{\beta-1}}{\mathcal{J}}$ for $\beta = i, i+2, i\pm 1$	$\frac{1}{\mathcal{J}}$	$\xi_{i+1} \Lambda_{i+1}(\mathbf{r}) + \xi_{i-1} \Lambda_{i-1}(\mathbf{r}) = 0$ $\xi_i \Lambda_i(\mathbf{r}) + \xi_{i+2} \Lambda_{i+2}(\mathbf{r}) = 0$
	Edge Singular Functions $\diamond$ ${}^e\Lambda_{i\pm 1}(\mathbf{r}) = (\nu \xi_i^{\nu-1} - 1) \Lambda_{i\pm 1}(\mathbf{r})$ ${}^e\mathbf{V}_{i+2}(\mathbf{r}) = (\xi_i^{\nu-1} - 1) \Lambda_{i+2}(\mathbf{r})$	$\frac{\nu \xi_i^{\nu-1} - 1}{\mathcal{J}}$	$\xi_{i+1} {}^e\Lambda_{i+1}(\mathbf{r}) + \xi_{i-1} {}^e\Lambda_{i-1}(\mathbf{r}) = 0$
Triangular Base The subscripts are counted modulo 3, for $i = 1, 2$ or 3	Regular Functions [4] $\Lambda_\beta(\mathbf{r}) = \frac{1}{\mathcal{J}} (\xi_{\beta+1} \ell_{\beta-1} - \xi_{\beta-1} \ell_{\beta+1})$ for $\beta = i, i\pm 1$	$\frac{2}{\mathcal{J}}$	$\xi_{i+1} \Lambda_{i+1}(\mathbf{r}) + \xi_{i-1} \Lambda_{i-1}(\mathbf{r}) + \xi_i \Lambda_i(\mathbf{r}) = 0$
	Vertex Singular Functions $\clubsuit$ ${}^v\Lambda_{i\pm 1}(\mathbf{r}) = \chi_a \Lambda_{i\pm 1}(\mathbf{r}) \mp \chi_b \frac{\xi_{i\mp 1} \ell_i}{\mathcal{J}}$ ${}^v\mathbf{V}_i(\mathbf{r}) = \chi_a \Lambda_i(\mathbf{r})$ with $\chi_a = (1 - \xi_i)^{\nu-1} - 1$ $\chi_b = (1 - \nu) (1 - \xi_i)^{\nu-2}$	$\frac{(1 + \nu) (1 - \xi_i)^{\nu-1} - 2}{\mathcal{J}}$	$\xi_{i+1} {}^v\Lambda_{i+1}(\mathbf{r}) + \xi_{i-1} {}^v\Lambda_{i-1}(\mathbf{r}) + \xi_i {}^v\mathbf{V}_i(\mathbf{r}) = 0$
	Edge Singular Functions $\diamond, \clubsuit$ ${}^e\Lambda_{i\pm 1}(\mathbf{r}) = (\nu \xi_i^{\nu-1} - 1) \Lambda_{i\pm 1}(\mathbf{r})$	$\frac{\nu (1 + \nu) \xi_i^{\nu-1} - 2}{\mathcal{J}}$	$\xi_{i+1} {}^e\Lambda_{i+1}(\mathbf{r}) + \xi_{i-1} {}^e\Lambda_{i-1}(\mathbf{r}) + \xi_i {}^g\Lambda_i(\mathbf{r}) = 0$
<p>♡ All the basis functions appearing in each row have identical surface divergence. In particular, for the singular functions, (1) yields <math>\nabla \cdot {}^e\Lambda_{i\pm 1}(\mathbf{r}) = \nabla \cdot {}^e\mathbf{V}_{i+2}(\mathbf{r}) = [\nu \chi^{\nu-1} - 1] / \mathcal{J}</math> for the quadrilateral base; <math>\nabla \cdot {}^v\Lambda_{i\pm 1}(\mathbf{r}) = \nabla \cdot {}^v\mathbf{V}_i(\mathbf{r}) = [(1 + \nu) \chi^{\nu-1} - 2] / \mathcal{J}</math> for the vertex singularity triangle, and <math>\nabla \cdot {}^e\Lambda_{i\pm 1}(\mathbf{r}) = [\nu (1 + \nu) \chi^{\nu-1} - 2] / \mathcal{J}</math> for the edge singularity triangle.</p> <p>◇ The edge singular functions are singular on the <math>i</math>-th edge (where <math>\xi_i = 0</math>), and vanish for <math>\nu = 1</math>.</p> <p>♣ The vertex singular functions are singular at the vertex <math>\xi_i = 1</math>, and vanish for <math>\nu = 1</math>.</p> <p>♠ The <i>ghost</i> function <math>{}^g\Lambda_i(\mathbf{r}) = (\nu \xi_i^{\nu-1} - 1) \Lambda_i(\mathbf{r})</math> appearing in the dependency relation at right does not belong to the edge singular triangular basis set because its divergence contains a non-physical <math>\xi_i^{\nu-2}</math> term. Although the divergence of the higher-order edgeless function <math>\xi_i {}^g\Lambda_i(\mathbf{r})</math> is physical (see (17)), the algorithm to construct independent higher-order edge-singular triangular bases has to discard all the functions obtained by multiplying the ghost function times a polynomial of the parent variables because of the reported dependency relation, or because the divergence of these functions contains non-physical hyper-singular terms.</p>			

## References

- [1] R. D. Graglia, D. R. Wilton, A. F. Peterson, "Higher order interpolatory vector bases for computational electromagnetics," *IEEE Trans. Antennas Propagat.*, vol. 45, no. 3, pp. 329-342, 1997.
- [2] R. D. Graglia, G. Lombardi, "Vector functions for singular fields on curved triangular elements, truly defined in the parent space," *Proc. IEEE AP-S Int. Symp. URSI Nat. Radio Science Meeting*, San Antonio, Texas, USA, Vol. 1, pp. 62-65, June 16-21, 2002.
- [3] R. D. Graglia, G. Lombardi, "Compatible singular vector functions for computational electromagnetics," *Atti della Fondazione Ronchi*, vol. 4, pp. 561-572, 2002, ISSN 0391 2051.
- [4] G. Lombardi, *Singular high-order complete vector functions for the analysis and design of electromagnetic structures with Finite Methods*, PhD Thesis, Politecnico di Torino, 2003.
- [5] R.D. Graglia, G. Lombardi, "Singular higher-order complete vector bases for Finite Methods," *IEEE Trans. Antennas Propagat.*, Vol. 52, No. 7, pp. 1672-1685, 2004.
- [6] R.D. Graglia, G. Lombardi, "Hierarchical singular vector bases for the FEM solution of wedge problems," *Proc. Int. Symp. on EM Theory* (invited), Pisa, Italy, May 2004.
- [7] R.D. Graglia, G. Lombardi, "Singular higher order divergence-conforming bases of additive kind and Moments Method applications to 3D sharp-wedge structures," *IEEE Trans. Antennas Propagat.*, due to appear in Dec 2008.

- [8] R.D. Graglia, G. Lombardi, *Numerical modeling procedure of singular vector physical quantities of a body, relative system and software product*, Patent Deposit, Sept. 5, 2003, Pub. N. WO/2005/024674, (<http://www.wipo.int/pctdb/en/wo.jsp?wo=2005024674>).

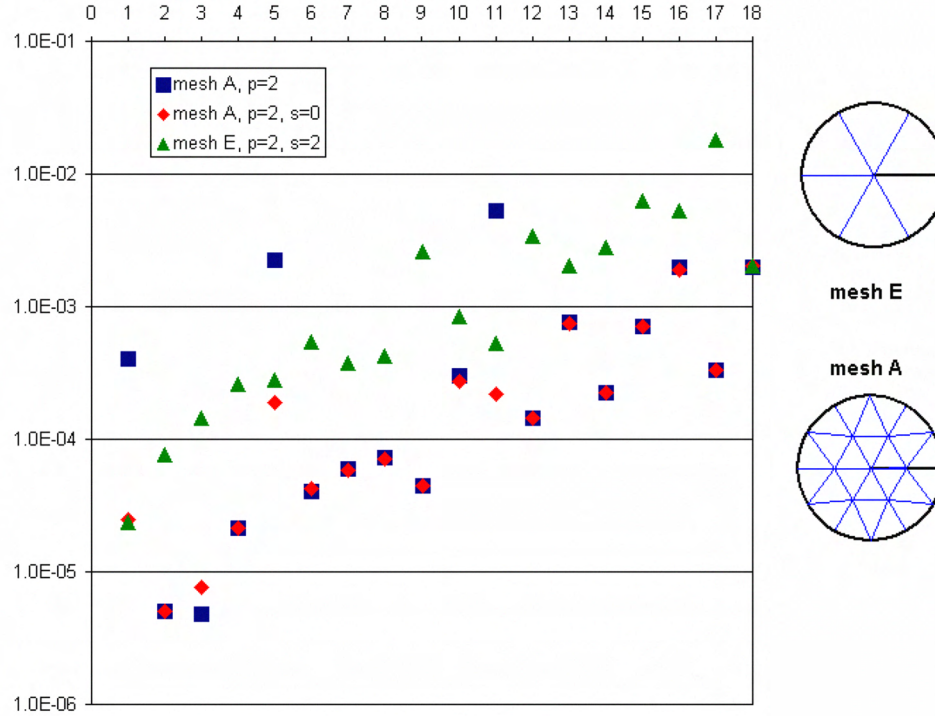


Fig.2: The relative errors of the computed square value of the longitudinal wavenumber for each of the first eighteen modes of the circular waveguide at  $k_0 a = 11$ , where  $a$  is the WG radius. Errors are reported in logarithmic scale for two different kind of meshes (Mesh A with 24 triangles and E with 6 triangles) and for different kind of bases (regular with  $p = 2$ , singular bases with  $p = 2$  and  $s = 0$  and finally singular bases with  $p = 2$  and  $s = 2$ ).

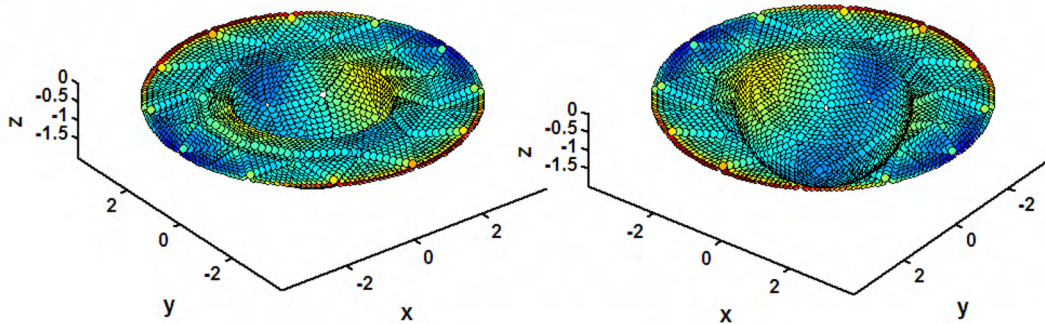


Fig.3: Current density induced on a half-sphere PEC shell of radius  $r$  terminated by a flat ring of external radius  $R$ , illuminated by a plane-wave propagating in the positive  $z$  direction. The  $z$ -axis passes through the center of the sphere. MoM results for  $k*r = 1.2566$ ;  $k*R = 2.5133$ . The figures show the magnitude of the total current induced on the shell seen from two different points of view.